

4.3 Multiple-Beam Interference

Consider the case shown in Figure 4.X1, where a plane wave with amplitude A illuminates a plane parallel plate at angle θ_1 . The plate is immersed in a lossless dielectric with refractive index n_1 . Similarly to the Fizeau interferometer described in Section 4.2.7, portion [1] of the light is reflected at interface I, and a portion is transmitted. The transmitted light can reflect from interface II and reemerge through interface I as beam [2]. Unlike the Fizeau interferometer, we now allow multiple reflections and transmissions from each interface. Fresnel reflection coefficients are r and r' , and transmission coefficients are t and t' . This section determines properties of this multiple-beam interference phenomenon, which leads to the concept of the *Fabry-Perot interferometer*.

If thickness d of the plate is constant, OPD between beams [2] and [3], as well as OPD between beams $[m]$ and $[m + 1]$, is the same as between beams [1] and [2]. This OPD is given by

$$\text{OPD} = 2n_2d \cos \theta_2, \quad (4.X1)$$

and the associated phase shift is given by

$$\delta = \frac{2\pi}{\lambda} \text{OPD} = \frac{2\pi}{\lambda} 2n_2d \cos \theta_2. \quad (4.X2)$$

Total reflected light for p reflections is given by

$$\begin{aligned} U_r(\delta) &= A \left(r + tt'r'e^{j\delta} + \dots + tt'r'^{(2p-3)}e^{j(p-1)\delta} \right) \\ &= A \left(r + tt'r'e^{j\delta} \sum_{m=0}^{p-2} r'^{2m} e^{jm\delta} \right) \\ &= A \left(r + tt'r'e^{j\delta} \frac{1 - r'^{2(p-1)}e^{j(p-1)\delta}}{1 - r'^2 e^{j\delta}} \right), \end{aligned} \quad (4.X3)$$

and total transmitted light is given by

$$\begin{aligned} U_t(\delta) &= Att' \left(1 + r'^2 e^{j\delta} + r'^4 e^{j2\delta} + \dots + r'^{2(p-1)} e^{j(p-1)\delta} \right) \\ &= Att' \frac{1 - r'^{2p} e^{jp\delta}}{1 - r'^2 e^{j\delta}}. \end{aligned} \quad (4.X4)$$

4.3.1 Stokes relations for lossless media

If there are no losses, a wave's propagation must be reversible. Figure 4.X2(a) shows a unit-amplitude plane wave reflected at interface I. Reversing both the reflected and transmitted waves produces the output shown in Fig. 4.X2(b), which must satisfy

$$\begin{aligned} tt' + r^2 &= 1 \\ tr' + rt &= 0 \quad , \end{aligned} \tag{4.X5}$$

so

$$\begin{aligned} tt' &= 1 - r^2 \\ r' &= -r \quad . \end{aligned} \tag{4.X6}$$

Therefore, if

$$tt' = T \tag{4.X7}$$

and

$$r^2 = r'^2 \quad , \tag{4.X8}$$

$$R + T = 1 \quad . \tag{4.X9}$$

4.3.2 Airy's formula

Simplification of Eq. (4.X3) is made by allowing $p \rightarrow \infty$ and substitution of Eq. (4.X6), such that

$$\begin{aligned} U_r(\delta) &= A \left(r - \frac{tt'r'e^{j\delta}}{1-r^2e^{j\delta}} \right) \\ &= Ar \left(\frac{1-r^2e^{j\delta} - tt'r'e^{j\delta}}{1-r^2e^{j\delta}} \right) \\ &= Ar \left[\frac{1-(r^2+tt')e^{j\delta}}{1-r^2e^{j\delta}} \right] \\ &= A \left[\frac{\sqrt{R}(1-e^{j\delta})}{1-Re^{j\delta}} \right] \quad . \end{aligned} \tag{4.X10}$$

The reflected irradiance is found from

$$\begin{aligned}
I_r(\delta) &= CU_r(\delta)U_r^*(\delta) \\
&= CA^2 \left[\frac{2R(1-\cos\delta)}{1+R^2-2R\cos\delta} \right], \tag{4.X11}
\end{aligned}$$

where $C = \frac{1}{2}cn_1\varepsilon_0$ is a constant. Since $1-\cos\delta = 2\sin^2\frac{\delta}{2}$,

$$I_r(\delta) = CA^2 \left[\frac{4R\sin^2\frac{\delta}{2}}{(1-R)^2 + 4R\sin^2\frac{\delta}{2}} \right], \tag{4.X12}$$

and

$$\frac{I_r(\delta)}{I_i} = \frac{4R\sin^2\frac{\delta}{2}}{(1-R)^2 + 4R\sin^2\frac{\delta}{2}}, \tag{4.X13}$$

where $I_i = CA^2$.

Similarly, for the transmitted light, Eq. (4.X4) becomes

$$U_t(\delta) = A \left(\frac{T}{1-Re^{i\delta}} \right), \tag{4.X14}$$

and the transmitted irradiance is

$$\begin{aligned}
I_t(\delta) &= CU_t(\delta)U_t^*(\delta) \\
&= CA^2 \left(\frac{T^2}{1+R^2-2R\cos\delta} \right). \tag{4.X15}
\end{aligned}$$

Therefore,

$$\frac{I_t(\delta)}{I_i} = \frac{T^2}{(1-R)^2 + 4R\sin^2\frac{\delta}{2}}. \tag{4.X16}$$

Equations (4.X13) and (4.X16) are known as Airy's formulas. Since there are no losses,

$$\frac{I_r(\delta)}{I_i} + \frac{I_t(\delta)}{I_i} = 1 \quad (4.X17)$$

Let F , the *coefficient of finesse*, be defined by

$$F = \frac{4R}{(1-R)^2} \quad (4.X18)$$

Note that F is always a positive number. After substitution of Eq. (4.X18), Airy's formulas become

$$\frac{I_r(\delta)}{I_i} = \frac{F \sin^2 \frac{\delta}{2}}{1 + F \sin^2 \frac{\delta}{2}} \quad (4.X19)$$

and

$$\frac{I_t(\delta)}{I_i} = \frac{1}{1 + F \sin^2 \frac{\delta}{2}} \quad (4.X20)$$

Changes in δ , that is d , λ , θ_1 or n_2 , change the reflected and transmitted irradiance periodically and therefore define *fringes* for observation in exactly the same way as described for a Fizeau interferometer in Section 4.2.7. For example, when $\delta = 2\pi m$, where m is an integer, reflected fringes exhibit zero irradiance. At these same values of δ , the transmitted fringes exhibit maximum irradiance. Unlike a Fizeau interferometer, multiple-beam interference caused by significant R now modifies fringe shape.

For example, notice that $F \rightarrow \infty$ as $R \rightarrow 1$. Therefore, for highly reflective surfaces,

$\frac{I_r(\delta)}{I_i} \rightarrow 1$, except where $\delta = 2\pi m$. That is, reflected fringes are mostly bright, except in

the narrow regions around $\delta = 2\pi m$, and fringe shape can be dramatically different than the cosine fringe patterns observed with Fizeau. Since transmitted and reflected irradiances are complementary, everywhere $\delta = 2\pi m$ produces a zero reflected fringe center, the transmitted fringe center exhibits a maximum value. For high R , the transmitted background is nearly zero and the maximum transmission is sharply peaked. These relationships are shown for $R = 0.04$ (Fizeau), 0.20 and 0.80 in Fig. 4.X3. Transmitted fringes are bright on a dark background as R increases, and reflected fringes are dark on a bright background. Notice that reflected fringe visibility is always $V = 1$, but $V = 1$ for transmitted fringes only when $R \rightarrow 1$.

4.3.3 Fringe sharpness and finesse

As R increases, minima of reflected fringes and maxima of transmitted fringes become sharper. A convenient way to express fringe sharpness is *finesse*, which is defined by

$$\mathcal{F} = \frac{\text{Separation of adjacent fringes}}{\text{width of fringe (half maximum)}} \quad (4.X21)$$

The transmitted fringes sketched in Fig. 4.X4 as a function of $\delta/2\pi$ exhibit a half-maximum fringe width of ε , which is found by finding δ at the half-maximum irradiance values such that

$$\frac{\delta_{1/2\max}}{2\pi} = m \pm \frac{\varepsilon}{2} \quad (4.X22)$$

If $R \rightarrow 1$ and F is very large, ε is small and Eq. (4.X20) becomes

$$\frac{1}{2} \approx \frac{1}{1 + F \sin^2 \frac{\delta_{1/2\max}}{2}} \quad (4.X23)$$

and solving for ε yields

$$\varepsilon = \frac{\sqrt{F}}{2\pi} \quad (4.X24)$$

Substitution of Eq. (4.X18) into Eq. (4.X24) and solving Eq. (4.X21)

$$\mathcal{F} = \frac{1}{\varepsilon} = \frac{\pi\sqrt{R}}{1-R} \quad (4.X25)$$

Notice that the *finesse*, which is a measure of fringe sharpness, only depends on the reflectivity R of the interfaces. Simply increasing

4.3.4 Absorbing coatings

In the presence of absorption in the coatings, Eq. (4.X9) must be modified to

$$R + T + A = 1 \quad (4.X26)$$

where A is the absorption through one interface. If Eq. (4.X16) is rewritten as

$$\frac{I_t(\delta)}{I_i} = \frac{T^2}{(1-R)^2} \frac{1}{1 + F \sin^2 \frac{\delta}{2}} \quad (4.X27)$$

substitution of $T = (1 - R) - A$ yields

$$\frac{I_t(\delta)}{I_i} = \left(1 - \frac{A}{1 - R}\right) \frac{1}{1 + F \sin^2 \frac{\delta}{2}} \quad (4.X28)$$

Therefore, one effect of an absorbing coating is to reduce the peak transmitted amplitude to

$$T_{\max} = \left(1 - \frac{A}{1 - R}\right)^2 = \left(\frac{1}{1 + A/T}\right)^2 \quad (4.X29)$$

As an example, if $R = 99.7\%$ and $A = 0.2\%$, $T = 0.1\%$ and $T_{\max} = 11\%$. However, if $R = 99.7\%$ and $A = 0.29\%$, $T = 0.01\%$ and $T_{\max} = 0.11\%$. Even though absorption is small, the large number of reflections makes the total loss large. In addition, the coatings may experience a phase change ϕ upon reflection from each surface, which modifies Eq. (4.X2) to

$$\delta = \frac{2\pi}{\lambda} \text{OPD} + 2\phi = \frac{2\pi}{\lambda} 2n_2 d \cos \theta_2 + 2\phi, \quad (4.X30)$$

so fringes are shifted according to 2ϕ . In reflection, the net result is that the interference fringes do not go to zero and visibility is reduced.

4.3.5 Fabry Perot

A basic Fabry Perot resonator etalon is shown in Fig. 4.X5. It consists of an extended incoherent source that is placed at the front focal plane of a collimating lens that provides a spectrum of plane-wave angles (θ_i) incident onto the Fabry Perot. The maximum angle of incidence is determined by the source radius and the lens focal length. Multiple-beam interference occurs for each plane-wave component illuminating the etalon. Depending on Eq. (4.X2) or (4.X30) for phase on reflection, the plane-wave component will be transmitted, reflected or part of both. The plane-wave components are then focused to the back focal plane of the second lens. Brightness of the focused spot from each plane-wave component depend on Eq. (4.X20) or (4.X30). Since the system is axially symmetric, the fringes are circular. With high R , the fringes are bright peaks on a dark background.

For a bright fringe of order m , Eq. (4.X30) is rearranged to

$$m = \frac{\delta}{2\pi} = \frac{\text{OPD}}{\lambda} + \frac{\phi}{\pi} = \frac{2n_2 d \cos \theta_2}{\lambda} + \frac{\phi}{\pi} \quad (4.X31)$$

Reflected and transmitted Fabry Perot fringes are shown in Fig. 4.X6 for low and high R . Notice that fringe distribution is exactly the same as for Haidinger's fringes. Like Haidinger's fringes, the center of the pattern exhibits maximum OPD. The only difference between Fabry Perot fringes and Haidinger's fringes in Section 4.2.6 is the fringe shape defined by finesse, which depends only on reflectivity.

4.3.5.1 Chromatic resolving power

If more than one wavelength is present in the source, each wavelength produces a separate fringe pattern in the observation plane. Irradiances from each fringe pattern add to produce total irradiance. In order to be resolved, the fringe patterns must be separated far enough to distinguish fringe peaks.

If a two-wavelength source has spectral components λ_1 and $\lambda_2 = \lambda_1 + \Delta\lambda$, the fringes are just resolved if, as shown in Fig. 4.X7, the half-widths of order m fringes from the two wavelengths just meet. In this case,

$$\frac{\delta_{1/2\max}}{2\pi} = \varepsilon \quad (4.X32)$$

From Eq. (4.X31),

$$\Delta\delta = -\frac{1}{\lambda} \delta \Delta\lambda \quad (4.X33)$$

Therefore,

$$\left| \frac{\lambda}{\Delta\lambda_{RES}} \right| = \frac{\delta/2\pi}{\Delta\delta_{1/2\max}/2\pi} = \frac{m}{\varepsilon} = m\mathcal{F} \quad (4.X34)$$

which is the *chromatic resolving power* of the etalon. The resolving power is a function of the order number and the reflectivity, where

$$\left| \frac{\lambda}{\Delta\lambda_{RES}} \right| = m\mathcal{F} = \frac{m\pi\sqrt{R}}{1-R} \quad (4.X35)$$

Near normal incidence, $m \approx 2n_2d/\lambda$, and resolving power $\approx 2n_2d\mathcal{F}/\lambda$.

For example, let $\mathcal{F} = 30$ ($R \sim 0.9$), $n_2d = 4$ mm and $\lambda = 500$ nm. Resolving power in this case is $\approx 5 \times 10^5$, and $\Delta\lambda_{RES} = 0.001$ nm.

4.3.5.2 Free spectral range

One might be tempted to assume that the chromatic resolving power can be increased indefinitely by increasing d . However, as d increases, separation of the modes decreases (fringes become more closely spaced). The point at which the m^{th} order of $\lambda_2 = \lambda_1 + \Delta\lambda$ falls on the $(m+1)^{\text{th}}$ order of λ_1 determines the limit of wavelength separation before ambiguities arise due to overlapping orders, as shown in Fig. 4.X8. At this limiting condition,

$$(m+1)\lambda_1 = m\lambda_2 = m(\lambda_1 + \Delta\lambda_{FSR}) , \quad (4.X36)$$

where $\Delta\lambda_{FSR}$ is the *free spectral range* of the etalon. Solution of Eq. (4.X36) results in

$$\Delta\lambda_{FSR} = \frac{\lambda}{m} = \frac{\lambda^2}{2n_2d \cos\theta_2} , \quad (4.X37)$$

so increasing the chromatic resolution by increasing d reduces free spectral range. Note that the ratio of the free spectral range and the resolving power is a constant, where

$$\frac{\Delta\lambda_{FSR}}{\Delta\lambda_{RES}} = \frac{\lambda/m}{\lambda\mathcal{F}/m} = \mathcal{F} = \frac{\pi\sqrt{R}}{1-R} . \quad (4.X38)$$

Near normal incidence,

$$\Delta\lambda_{FSR} = \frac{\lambda^2}{2n_2d} , \quad (4.X39)$$

and

$$\Delta\nu_{FSR} = \frac{c}{2n_2d} . \quad (4.X40)$$

4.3.5.3 Scanning Fabry Perot

The scanning Fabry Perot is useful when measuring a few discrete wavelengths, like with a laser beam. As shown in Fig. 4.X9, the flat mirrors are mounted such that one mirror moves to scan δ by changing d with an applied voltage that is synchronized to an oscilloscope trace. When δ matches an transmission peak for a wavelength in the source, the detector responds with a rise in current and corresponding increase in voltage on the oscilloscope display.

Since, for a given fringe,

$$2d = m\lambda , \quad (4.X41)$$

$$2\Delta d = m\Delta\lambda = \frac{2d}{\lambda} \Delta\lambda \quad (4.X42)$$

or

$$\frac{\Delta d}{d} = \frac{\Delta\lambda}{\lambda} \quad (4.X43)$$

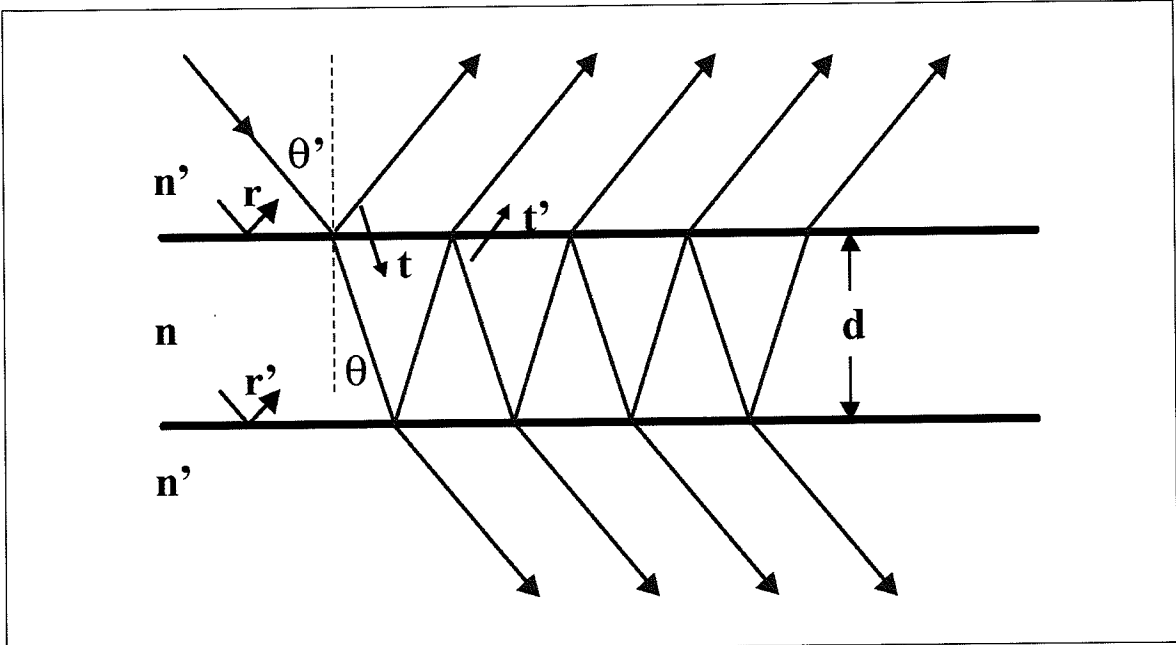


Figure 4.X1 Geometry for multiple-beam interference.

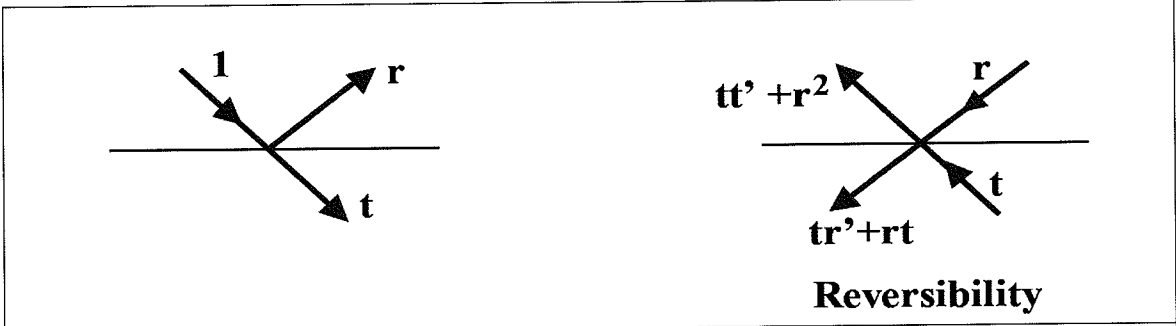
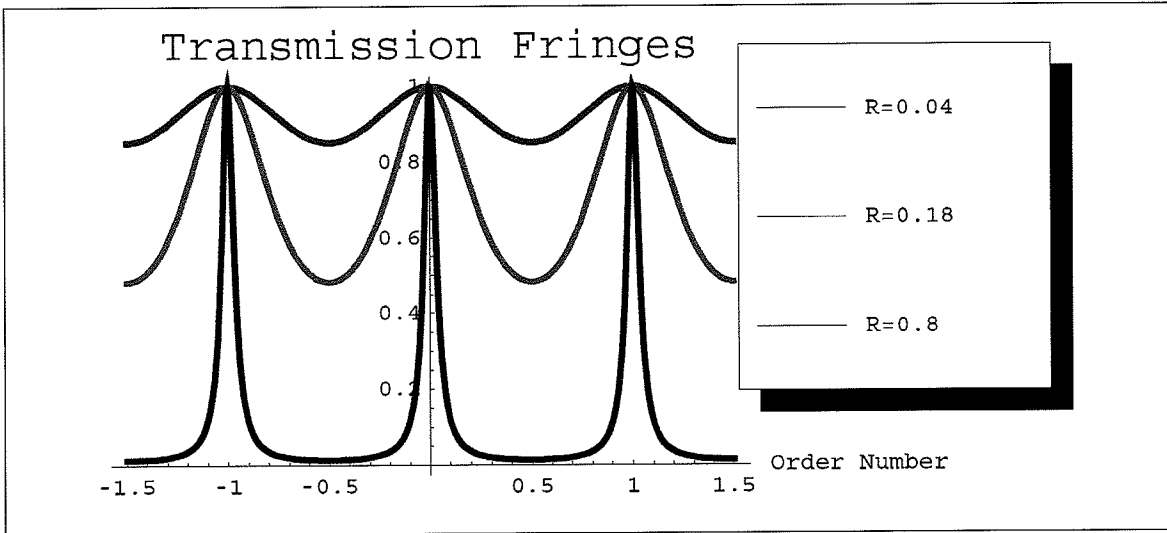
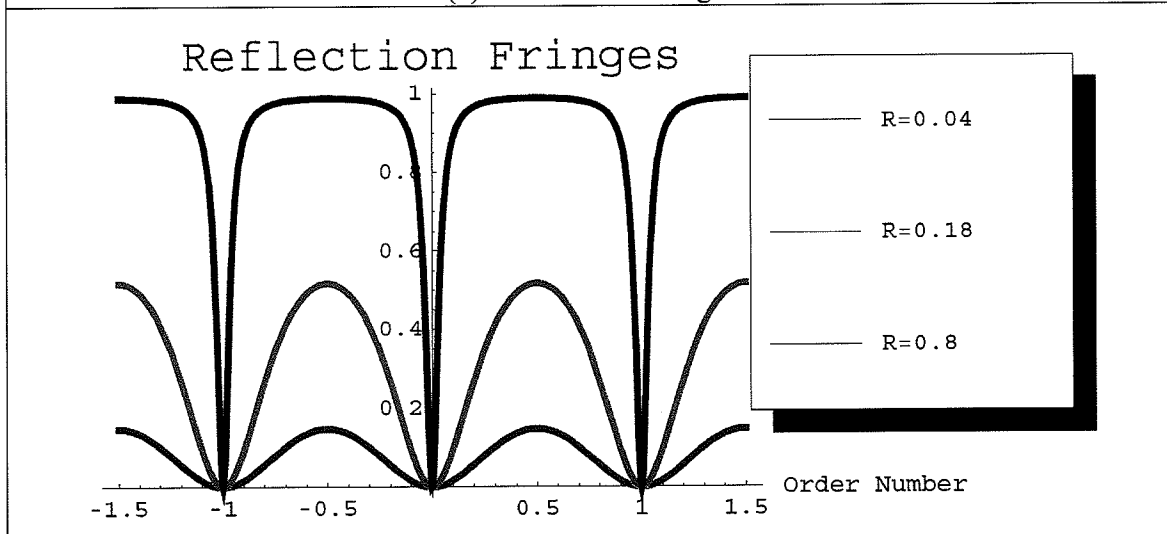


Figure 4.X2 Stokes parameters



(a) Transmitted fringes



(b) Reflected fringes

Figure 4.X3 Multiple-beam fringe shapes versus reflectivity R . (a) Transmitted (b) Reflected.

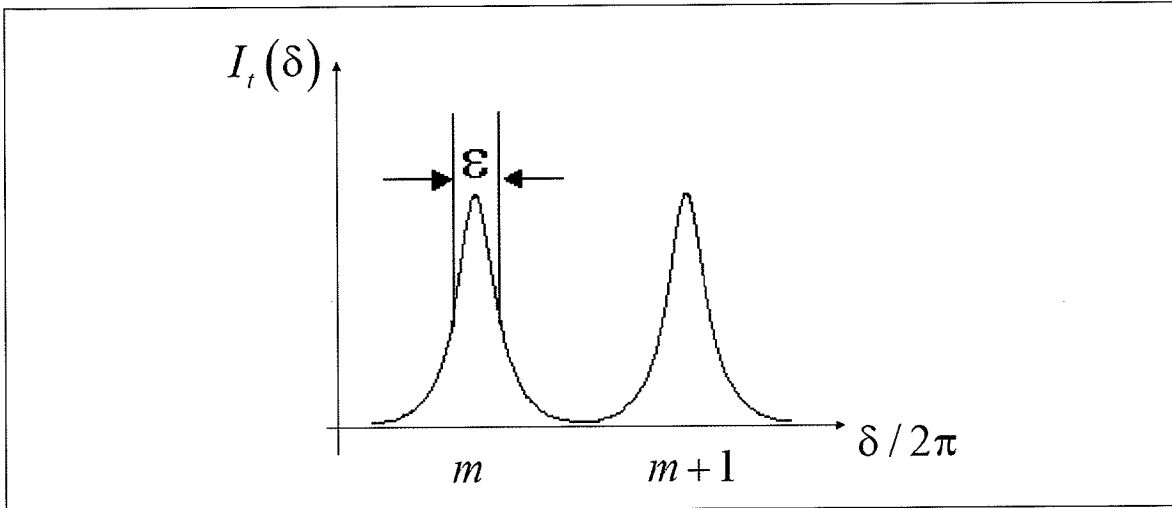


Figure 4.X4 Finesse and fringe sharpness.

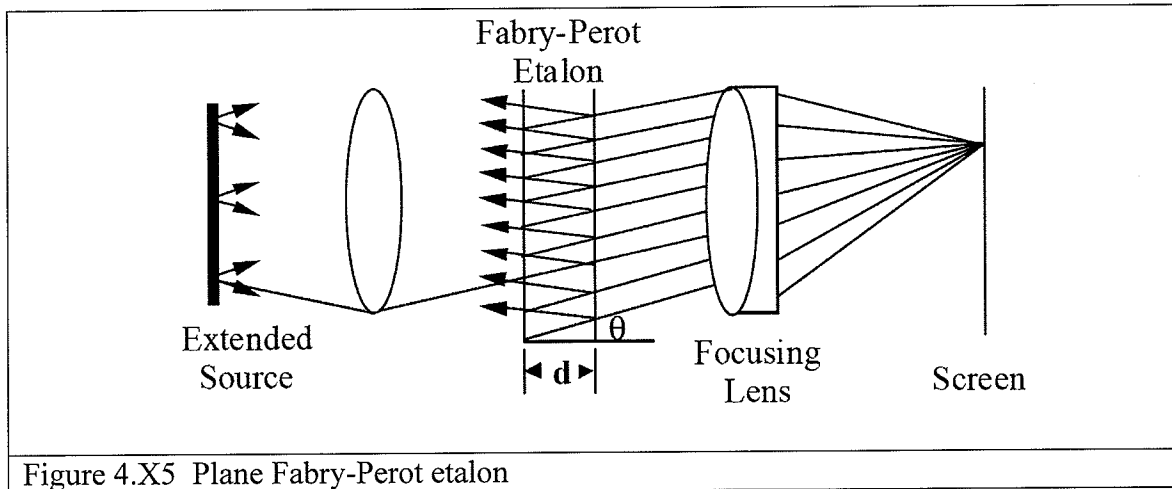


Figure 4.X5 Plane Fabry-Perot etalon

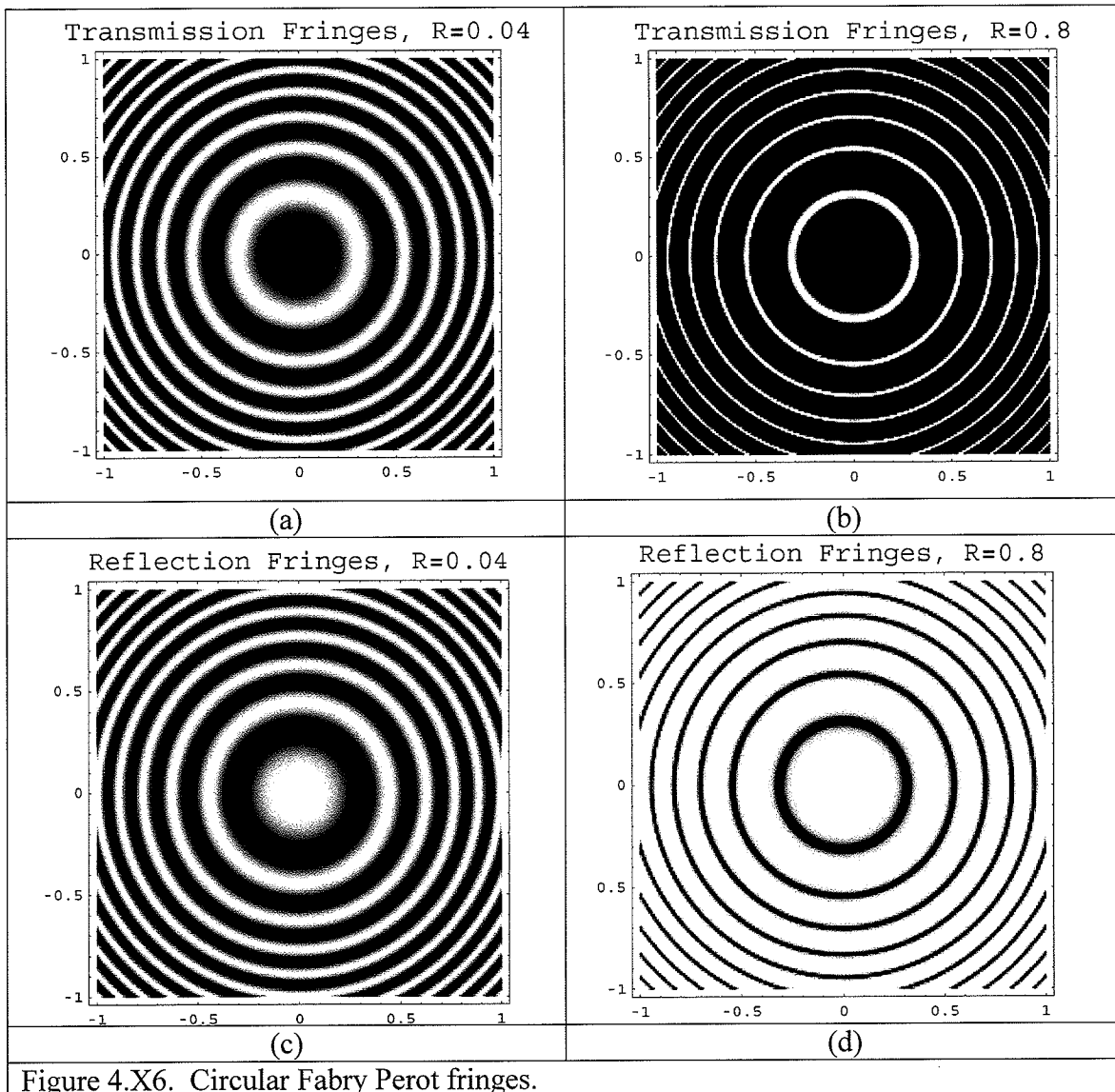


Figure 4.X6. Circular Fabry Perot fringes.

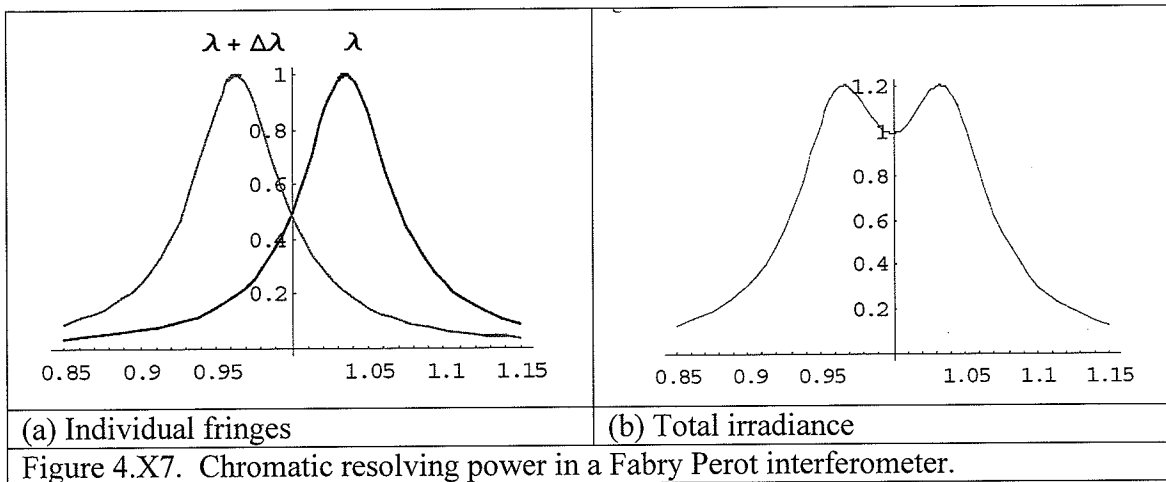


Figure 4.X8 Free spectral range in a Fabry Perot interferometer.
--

